Dynamics of a Two-Dimensional System of Quantum Dipoles

F. Mazzanti,[1] R. E. Zillich,[2] G. E. Astrakharchik,[1] and J. Boronat[1]

[1]Departament de Física i Enginyeria Nuclear, Campus Nord B4-B5, Universitat Politècnica de Catalunya, E-08034 Barcelona, Spain
[2]Institut für Theoretische Physik, Johannes-Kepler Universität, Altenbergerstr. 69, 4040 Linz, Austria

(Received 27 October 2008; published 20 March 2009)

A detailed microscopic analysis of the dynamic structure function $S(k, \omega)$ of a two-dimensional Bose system of dipoles polarized along the direction perpendicular to the plane is presented and discussed. Starting from ground-state quantities obtained using a quantum diffusion Monte Carlo algorithm, the density-density response is evaluated in the context of the correlated basis functions (CBF) theory. CBF predicts a sharp peak and a multiexcitation component at higher energies produced by the decay of excitations. We discuss the structure of the phonon-roton peak and show that the Feynman and Bogoliubov predictions depart from the CBF result already at low densities. We finally discuss the emergence of a roton in the spectrum, but find the roton energy not low enough to make the system unstable under density fluctuations up to the highest density considered that is close to the freezing point.

DOI: 10.1103/PhysRevLett.102.110405 PACS numbers: 03.75.Hh

The recent experimental achievements in trapping clouds of dipolar atoms [1,2] have opened the possibility of studying the static and dynamic properties of quantum systems governed by long range dipolar interactions. In particular, the realization of Bose-Einstein condensates (BECs) of chromium atoms [3], which has a large magnetic dipole moment, has stimulated great interest in understanding the properties of dipolar quantum systems at ultralow temperatures. In actual experiments conducted on BECs, the dipolar interaction coexists with other two-body interatomic potentials whose scattering length can be tuned by exploiting Feshbach resonances. In the low density limit the scattering length of the latter potential can take arbitrary values, and particularly it can be tuned to zero, leaving the dipole-dipole interaction as the only relevant potential. Additionally, polar gases are very rich from a physical point of view since they present strong resemblances with other interesting condensed matter systems such as superfluids or Mott insulators. Bilayer excitons [4] and more recently polar molecules [5] can possess strong dipole moments dominating their static and dynamic properties.

The ground-state properties of a trapped condensate of dipoles was analyzed in Ref. [6] at a mean-field level. BECs of dipoles in cigar-shaped and pancake geometries at finite temperatures where analyzed by means of the Path Integral Monte Carlo method in Ref. [7]. Other, more complex situations, where the scattering length varies with the dipole moment, have also been analyzed [8]. Recent studies on infinite 2D systems of dipoles have been carried out in an effort to understand the limiting behavior of a BEC of dipoles in a pancake geometry where the confinement in one direction is tight [9].

The anisotropy of the dipole-dipole interaction makes the ground-state and excitation spectrum depend strongly on the confining geometry [10–13]. In particular, the fact that the dipole-dipole potential can be attractive or repulsive has a direct impact on the elementary excitation spectrum, which can exhibit a roton minimum as happens in other, strongly correlated systems like ^{4}He. The roton excitation described by mean-field is very different in nature from the rotons in ^{4}He where it is not a signature of an instability due to *attractive* interaction, but rather a consequence of the near-order induced by the strongly *repulsive* core of the He-He interaction. For these systems many-body theories capable of dealing with strong correlations were developed long ago, both for homogeneous [14–16] and inhomogeneous [17] phases. These theories predict a spectrum $\epsilon(k)$ and a dynamic structure function $S(k, \omega)$ that are more accurate and have a richer structure than the ones provided by the Bjil-Feynman or Bogoliubov approximations, which only predict delta peaks in the (k, ω) plane corresponding to single-quasiparticle modes of infinite lifetime.

In this work we present a microscopic calculation of $\epsilon(k)$ and $S(k, \omega)$ for an infinite two-dimensional system of bosonic dipoles that are polarized along the direction perpendicular to the plane. The model Hamiltonian reads

$$H = -\frac{\hbar^2}{2m}\sum_j \nabla_j^2 + \frac{C_{dd}}{4\pi}\sum_{i<j}\frac{1}{|\mathbf{r}_i - \mathbf{r}_j|^3} \qquad (1)$$

with m the mass of the dipoles, $\{\mathbf{r}_j\}$ their position coordinates and C_{dd} the coupling constant that depends on the dipole moment. In the following we will use dimensionless quantities, introducing a characteristic length scale $r_0 = mC_{dd}/(4\pi\hbar^2)$ and a characteristic energy scale $E_0 = \hbar^2/mr_0^2$. We build on previous work by some of us [9], where ground-state energies, pair distribution, and the static structure factor $S(k)$ were obtained in an essentially exact form by diffusion Monte Carlo (DMC) simulations. In the present work, we apply a formalism based on correlated basis functions (CBF) [14], using DMC ground-state results for $S(k)$ as an input. The CBF formal-

ism constitutes a framework for calculating dynamic properties of strongly correlated systems. In the present work we use an implementation which can be derived by Brillouin-Wigner perturbation theory [15].

The CBF formalism provides a model for the linear response function from which $S(k, \omega)$ is obtained as

$$S(k, \omega) = -\frac{1}{\pi} \mathrm{Im} \frac{S(k)}{\hbar\omega - \epsilon_F(k) - \Sigma(k, \omega) + i\eta}, \quad (2)$$

with $\epsilon_F(k) = \hbar^2 k^2 / 2mS(k)$ the Bjil-Feynman spectrum [18]. The self-energy term $\Sigma(k, \omega)$ contains all the information about the response that is not present in the Feynman mode,

$$\Sigma(k, \omega) = \frac{1}{2} \int \frac{d\mathbf{p} d\mathbf{q}}{(2\pi)^3 \rho} \frac{\delta(\mathbf{k} + \mathbf{p} + \mathbf{q}) |V_3(\mathbf{k}, \mathbf{p}, \mathbf{q})|^2}{\hbar\omega - \epsilon_F(p) - \epsilon_F(q) + i\zeta}, \quad (3)$$

where the matrix element $V_3(\mathbf{k}, \mathbf{p}, \mathbf{q})$, written in terms of the direct correlation function $X(k) = 1 - 1/S(k)$, reads

$$V_3(\mathbf{k}, \mathbf{p}, \mathbf{q}) = \frac{\hbar^2}{2m} \sqrt{\frac{S(p)S(q)}{S(k)}} [\mathbf{k} \cdot \mathbf{p} X(p) + \mathbf{k} \cdot \mathbf{q} X(q) - k^2 u_3(\mathbf{k}, \mathbf{p}, \mathbf{q})], \quad (4)$$

which represents a three-phonon scattering vertex that allows single excitations to decay into two. In this expression, $u_3(\mathbf{k}, \mathbf{p}, \mathbf{q})$ is a ground-state triplet correlation that has been taken to be the convolution approximation to its optimal form [19]. From Eq. (2) we see that the spectrum of elementary excitations $\epsilon(k)$ at fixed k can be obtained by solving the equation $\hbar\omega - \epsilon_F(k) - \Sigma(k, \omega) = 0$ for $\hbar\omega = \epsilon(k)$. CBF belongs to a family of theories predicting a real valued spectrum $\epsilon(k)$. If a solution exists (and thus $\mathrm{Im}\Sigma(k, \omega) = 0$), the CBF response shows a delta peak of strength $Z(k)$ at the energy $\hbar\omega = \epsilon(k)$ with $Z(k) = S(k)|1 - d\mathrm{Re}\Sigma(k, \omega)/d\omega|^{-1}_{\omega=\epsilon(k)}$ the spectral weight of the peak. A small but finite $\mathrm{Im}\Sigma(k, \omega)$ leads to damping (decay of excitations) seen as an homogeneously broadened peak centered at $\epsilon(k)$, which is obtained by solving $\hbar\omega - \epsilon_F(k) - \mathrm{Re}\Sigma(k, \omega) = 0$ in $S(k, \omega)$. That is the case for instance when the excitation spectrum $\epsilon(k)$ is monotonically increasing and concave [$\epsilon''(k) > 0$] [17], where it is possible to conserve energy and momenta in the scattering process of one excitation decaying in two. Finally, if $\mathrm{Im}\Sigma(k, \omega)$ is large (on the order of $\hbar\omega$), we do not get a well-defined dispersion anymore. Regions where $\mathrm{Im}\Sigma(k, \omega)$ is large are referred to as the multiexcitation continuum. Note that if we set $\Sigma(k, \omega) = 0$, we obtain the Feynman approximation for the dynamic structure function, $S(k, \omega) = S(k)\delta(\hbar\omega - \epsilon_F(k))$. The CBF formalism has been extensively applied to liquid ^{4}He [20] and is known to describe well most of the features of $S(k, \omega)$. Although not exact, $\epsilon(k)$ is a significant improvement over the Feynman spectrum $\epsilon_F(k)$. It is also important to point out that, in CBF, $S(k, \omega)$ exactly fulfills the lowest order energy-weighted sum rules [21].

Figure 1 shows a color-coded map of the dynamic structure function on a logarithmic scale at four different densities. We plot $nr_0^2 S(k, \omega)$ as a function of scaled energies $\hbar\omega/(nr_0^2)$ and scaled momenta $k/n^{1/2}$ as we found in Ref. [9] that all these quantities scale better with the density. The inclusion of the CBF self-energy leads to a dispersion $\epsilon(k)$ lower than the Feynman mode. The excitation spectrum $\epsilon(k)$ is seen as a sharp peak in Fig. 1 for all but the lowest density. We find that there is no decay for these excitations of energy $\epsilon(k)$ [for the purpose of illustration, $S(k, \omega)$ has been broadened by $\eta = 0.15E_0$ in order to make the excitation easier to identify]. Most notably, the $\epsilon(k)$ mode starts to exhibit a nonmonotonic behavior as the density increases, thus forming a roton at sufficiently high density. The CBF prediction of the roton energy is significantly lower than the Feynman prediction. We stress again that the formation of this roton is an effect of the strong correlation in the plane rather than due to the emergence of an instability of the system. In fact, 2D rotons have been identified experimentally in neutron scattering measurements on liquid ^{4}He adsorbed on graphite [17] and in aerogel and vycor [22]. For the rest of the Letter we will refer to the $\epsilon(k)$ mode as the phonon-roton mode also for low densities without roton.

Unlike the Feynman mode, the CBF mode does not have the full spectral weight, $Z(k) < S(k)$, because $S(k, \omega)$ has, in addition to the elementary excitation mode, also higher energy features, as discussed below. For all densities, the phonon-roton dispersion is eventually "absorbed" [$Z(k) \to 0$] into the continuum of $S(k, \omega)$ at sufficiently large wave number k such that there is no well-defined dispersion relation for higher k's. For the highest density

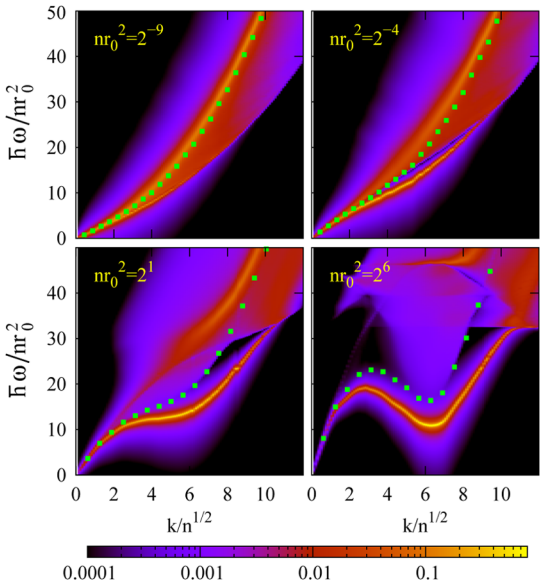

FIG. 1 (color online). $nr_0^2 S(k, \omega)$ of a 2D system of dipoles at four different densities. Notice that the CBF delta peak has been broadened into a Lorentzian shape in order to make it easier to identify. The green squares show the Feynman spectrum $\epsilon_F(k)$.

$nr_0^2 = 2^6$ shown in Fig. 1, the dispersion bends to a constant value at about $k/n^{1/2} = 10$, thus forming a plateau before losing all spectral weight. Notice that this feature is absent in the Feynman mode, which keeps its strength $Z(k) = S(k)$ all along the curve (thus approaching 1 at high k) and becomes the free excitation spectrum $t(k) = \hbar^2k^2/2m$ for large k. Such a plateau has been observed experimentally for 3D ^{4}He, where its energy is precisely twice the roton energy which indicates that it decays into two rotons. This interpretation is confirmed by the CBF approximation, although quantitatively the plateau is situated at twice the roton energy in Feynman approximation. This prediction can possibly be improved by including fluctuations in the triplet correlation terms [23].

At energies above the phonon-roton dispersion, a multiexcitation background emerges (seen as the red to orange contributions in Fig. 1). Exciting the system at such high energies leads to fast decay into two lower energy excitations. However, at low density we still observe a dispersionlike feature, that is slightly broadened. Figure 2 shows a plot of $S(k, \omega)$ at the (low) density $nr_0^2 = 2^{-7}$ and for $k/n^{1/2} = 6.4$, very close to the scaled wave number of the roton at higher density. The sharp peak at $\hbar\omega/E_0 \approx 15$ corresponds to the CBF phonon-roton mode $\epsilon(k)$, (again broadened slightly for better visibility), while the remaining structure at higher energies is the multiexcitation contribution. The position of the Feynman mode $\epsilon_F(k)$ and the Bogoliubov mode $\epsilon_B(k)$ [24,25] [the latter in terms of the s-wave scattering length of the interaction $a = \exp(2\gamma)r_0$ and the Euler constant $\gamma = 0.5772\ldots$] [9],

$$\epsilon_B(k) = \sqrt{\left(\frac{\hbar^2k^2}{2m}\right)^2 + \left(\frac{\hbar^2k}{2m}\right)^2 \frac{16\pi n}{|\ln(na^2)|}}, \qquad (5)$$

are shown with arrows. It can be clearly seen that despite the low density, the Feynman and Bogoliubov modes differ from each other and from the CBF prediction, which is closer to the exact $S(k, \omega)$. The difference between the Feynman and Bogoliubov predictions are due to the fact that the Bogoliubov spectrum can be seen as an approximation to the Feynman spectrum when the actual interaction potential is replaced by a (density dependent) contact interaction, while the Feynman excitation is an approximation to the CBF result when the self-energy term is discarded. For the density and wave number considered in Fig. 2, the maximum of the broad CBF peak has about 80% of the total spectral strength and is located between the Feynman and Bogoliubov energies.

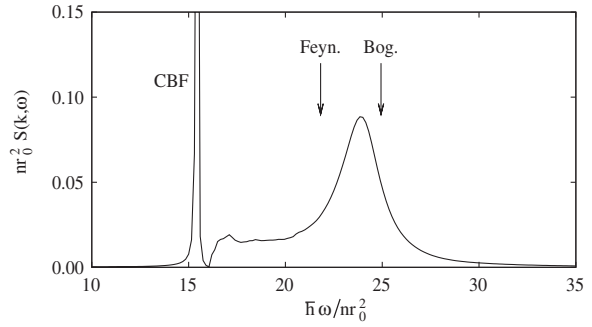

FIG. 2. $nr_0^2S(k, \omega)$ for $k/n^{1/2} = 6.4$ at the density $nr_0^2 = 2^{-7}$. The arrows point the position of the corresponding Bogoliubov and Feynman peaks.

At the low density of Fig. 2, the multiexcitation contribution predicted in CBF theory can be identified with the Bogoliubov mode, because it is a well-defined, although broad peak, consistent with a quasiparticle picture, at an energy close to the Bogoliubov mode. As the density increases, however, this peak loses spectral weight in favor of the phonon-roton excitation. This is shown in Fig. 3 for two momenta and several densities spanning the range $nr_0^2 = 2^{-14}$ to $nr_0^2 = 2^8$ (the later close to the freezing density $nr_0^2 = 290$ [9]), where $\epsilon_B(k)$ and $\epsilon_F(k)$ are shown with star and square symbols, respectively. Note that the quasiparticle picture consistent with the Bogoliubov and Feynman approximation only holds at low densities, and that as soon as the density increases above some value around $nr_0^2 = 2^{-8}$, $\epsilon_B(k)$ and $\epsilon_F(k)$ depart from each other and from the CBF prediction. At even higher densities the Bogoliubov approximation does not apply anymore, as much of the spectral strength shifts to the phonon-roton branch while the multiexcitation component spreads over a wider range of energies. Actually the bare Bogoliubov spectrum $\epsilon_B(k)$ diverges at the value $nr_0^2 \approx 2^{-3.33}$, corresponding to $na^2 = 1$ [see Eq. (5)]. On the other hand, the physical interpretation of the Feynman mode changes as

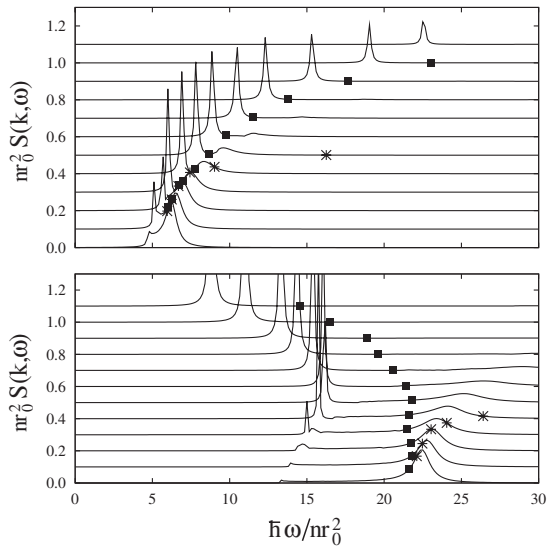

FIG. 3. $nr_0^2S(k, \omega)$ for the momenta $k/n^{1/2} = 3.0$ and $k/n^{1/2} = 6.4$ (close to the roton wave number) as a function of the energy (upper and lower panels, respectively). Different lines represent increasing densities from bottom to top. The lowest line corresponds to $nr_0^2 = 2^{-14}$, the next one to $nr_0^2 = 2^{-12}$, the following to $nr_0^2 = 2^{-10}$ and so on, up to the last one where $nr_0^2 = 2^8$. Notice that $S(k, \omega)$ has been shifted upwards with increasing density. The squares and stars show the Feynman and Bogoliubov spectrum, respectively.

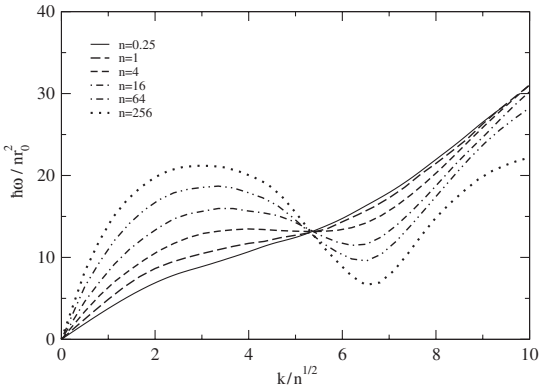

FIG. 4. Phonon-roton spectra $\epsilon(k)/nr_0^2$ for various densities ranging from $nr_0^2 = 2^8$ (upper curve at low wave number), $nr_0^2 = 2^6$, $nr_0^2 = 2^4$, ..., down to $nr_0^2 = 2^{-2}$.

nr_0^2 increases, moving from the Bogoliubov quasiparticles picture in the $nr_0^2 \to 0$ limit to qualitatively describe the phonon-roton peak. We have checked that analogous conclusions hold for other wave numbers, with the phonon-roton peak and the multiexcitation component being closer at low densities and decreasing wave number. Only in the $k \to 0$ limit the Feynman and CBF approximations yield the same dispersion, namely $\hbar kc$, where c is the speed of sound.We end the discussion by going back to the analysis of the phonon-roton branch $\epsilon(k)$ as a function of the density. Figure 4 shows the energy $\epsilon(k)$ of the CBF phonon-roton mode at several densities. The spectrum of elementary excitations is monotonically increasing for low n until it develops a rotonlike minimum at a fairly high critical density n_r of the order of $n_r r_0^2 \approx 2^2$. Surprisingly, all curves seem to intersect at the same point, $k/n^{1/2} \approx 5$, using our scaling of k. This point coincides with the point at which the roton first emerges, taken as the k value at which the phonon-roton line at the density n_r has zero slope. Notice also that not even at the highest density considered $nr_0^2 = 2^8$, close to solidification, the roton approaches the zero energy axis, thus indicating that the 2D system of dipoles analyzed is always stable under density fluctuations in this phase.

To summarize, we have carried out a microscopic calculation of the dynamic structure function of a gas of dipoles in 2D using the formalism of correlated basis functions. For that and as an input, we used ground-state quantities obtained from a diffusion Monte Carlo simulation of the system. The combination of the DMC method, which is able to produce essentially exact results for the ground state, and the CBF theory, which is a well-founded microscopic theory of elementary excitations, allows for a very accurate description of the dynamic response function in a wide range of densities. We report predictions for the phonon-roton branch that coincide with the Feynman and Bogoliubov modes only at very low densities, pushing it down to lower energies as nr_0^2 increases. The CBF method also predicts a multiexcitation component that is absent in the other two approximations. We find that a roton emerges at a density of about $nr_0^2 = 2^2$, and that the energy of the roton decreases with increasing density, but not to the point of making the system unstable against density fluctuations. We are currently working on the extension of this study to a pancake geometry using the inhomogeneous version of the CBF theory and DMC simulations to study the stability in a trap against collapse in a quantitatively accurate form.

R. E. Z. thanks E. Krotscheck for helpful discussions. This work has been partially supported by Grants No. FIS2005-03142 and FIS2005 from DGI (Spain), and Grants 2005SGR-00343 and 2005SGR-00779 from the *Generalitat de Catalunya*.

[1] C. C. Bradley *et al.*, Phys. Rev. Lett. **78**, 985 (1997).
[2] T. Lahaye *et al.*, Nature (London) **448**, 672 (2007).
[3] A. Griesmaier *et al.*, Phys. Rev. Lett. **94**, 160401 (2005).
[4] S. De Palo *et al.*, Phys. Rev. Lett. **88**, 206401 (2002).
[5] K.-K. Ni *et al.*, Science **322**, 231 (2008).
[6] L. Santos, G. V. Shlyapnikov, P. Zoller, and M. Lewenstein, Phys. Rev. Lett. **85**, 1791 (2000).
[7] K. Nho and D. P. Landau, Phys. Rev. A **72**, 023615 (2005).
[8] S. Ronen *et al.*, Phys. Rev. A **74**, 033611 (2006).
[9] G. E. Astrakharchik *et al.*, Phys. Rev. Lett. **98**, 060405 (2007).
[10] L. Santos *et al.*, Phys. Rev. Lett. **90**, 250403 (2003).
[11] D. H. J. O'Dell *et al.*, Phys. Rev. Lett. **90**, 110402 (2003).
[12] S. Ronen *et al.*, Phys. Rev. Lett. **98**, 030406 (2007).
[13] R. M. Wilson *et al.*, Phys. Rev. Lett. **100**, 245302 (2008).
[14] E. Feenberg, *Theory of Quantum Fluids* (Academic Press, New York, 1967 and 1969).
[15] C. C. Chang and C. E. Campbell, Phys. Rev. B **13**, 3779 (1976).
[16] H. W. Jackson and E. Feenberg, Rev. Mod. Phys. **34**, 686 (1962).
[17] B. E. Clements *et al.*, Phys. Rev. B **50**, 6958 (1994).
[18] R. P. Feynman and M. Cohen, Phys. Rev. **102**, 1189 (1956).
[19] E. Krotscheck, Phys. Rev. B **33**, 3158 (1986).
[20] V. Apaja and E. Krotscheck, in *Microscopic Approaches to Quantum Liquids in Confined Geometries*, edited by E. Krotscheck and J. Navarro (World Scientific, Singapore, 2002).
[21] H. W. Jackson, Phys. Rev. A **9**, 964 (1974).
[22] B. Fåk *et al.*, Phys. Rev. Lett. **85**, 3886 (2000).
[23] E. Krotscheck and C. E. Campbell, in *Proceedings of the 14th International Conference on Recent Progress in Many-Body Theories*, edited by J. Boronat, G. E. Astrakhachik, and F. Mazzanti (World Scientific, Singapore, 2008).
[24] M. Schick, Phys. Rev. A **3**, 1067 (1971).
[25] A. Posazhennikova, Rev. Mod. Phys. **78**, 1111 (2006).